An Ultrasensitive Bacterial Motor Revealed by Monitoring Signaling Proteins in Single Cells

Philippe Cluzel,[1]* Michael Surette,[2] Stanislas Leibler[1]

Understanding biology at the single-cell level requires simultaneous measurements of biochemical parameters and behavioral characteristics in individual cells. Here, the output of individual flagellar motors in *Escherichia coli* was measured as a function of the intracellular concentration of the chemotactic signaling protein. The concentration of this molecule, fused to green fluorescent protein, was monitored with fluorescence correlation spectroscopy. Motors from different bacteria exhibited an identical steep input-output relation, suggesting that they actively contribute to signal amplification in chemotaxis. This experimental approach can be extended to quantitative in vivo studies of other biochemical networks.

Biochemical networks have been the object of intensive experimental and theoretical studies. The understanding of their functioning relies mainly on data collected from populations rather than from single cells (*1*). When phenotypic variability is observed, however, single-cell measurements become indispensable (*2*). Here, we present an experimental method to correlate intracellular enzyme concentrations with behavioral characteristics in single cells. We adopted this approach to characterize, in *Escherichia coli*, the output device of the chemotactic network—an individual flagellar motor. Measuring the input-output characteristics of motors may be relevant for understanding the high amplification gain in the chemotactic sensory system (*3*). In measurements over bacterial populations (*4–6*), its input-output characteristic was found to be too mild to contribute substantially to the observed high amplification of the chemotaxis system. Several molecular mechanisms of amplification, such as clustering of receptors (*7*), were thus subsequently proposed.

E. coli is propelled by several flagella. Each flagellum rotates under the action of a rotary motor (*8*). When motors rotate counterclockwise (CCW), the flagella form a bundle and the bacterium swims smoothly (*9*); when motors rotate clockwise (CW), the bundle flies apart and the bacterium tumbles in an erratic fashion. Tumble events randomize the cell trajectory, and the modulation of their occurrence allows bacteria to perform chemotaxis by swimming toward attractants or away from repellents (*10*). Specific receptors detect changes of environmental chemical concentrations and send a signal through the chemotactic network to the flagellar motors. CheY-phosphate (CheY-P) is the output of the signal transduction network. CheY-P binds preferentially to the motor (*11*), and the CW bias of the flagellar motors, that is, the fraction of time that a single motor spends rotating in the CW direction, increases with CheY-P concentration [CheY-P] (*4*).

The experiment described here was designed to determine, in single cells, the bias of individual motors as a function of [CheY-P]. The intracellular concentration of chemotactic proteins fused to the green fluorescent protein (GFP) was measured directly in individual cells of *E. coli*. To control the expression levels of CheY-P, we transformed the PS2001 strain of *E. coli*, lacking the *cheY* gene (*12*), with an inducible lac promoter plasmid expressing a *cheY-gfp* fusion gene (*13*). To our knowledge, there is no technique for measuring the phosphorylation levels of CheY-GFP in vivo. Therefore, a reliance on in vitro kinase activity measurements (*12*) reinforced the hypothesis that the entire pool of CheY molecules is phosphorylated in the transformed PS2001 strain (*4*).

Cell bodies were immobilized and specifically attached onto microscope slides so that some of the flagella were free to rotate. Rotating flagella were marked with latex microbeads to visualize their rotation with a dark-field illumination. The CW bias was obtained from analysis of video recordings (Fig. 1A).

An apparatus based on the fluorescence correlation spectroscopy (FCS) technique (*14–18*), mounted on an inverted microscope (Fig. 1A), allowed us to measure in vivo the concentration of proteins fused to GFP and to monitor behavioral cellular characteristics (CW bias). We focused the incident excitation laser beam onto a small volume of the cell and collected, in a confocal geometry, the fluorescence light emitted by the GFP molecules. Because the fluorescence intensity did not depend on the position of the illumination spot, we supposed that the expression of CheY-GFP was homogenous within a single cell. We obtained absolute concentration of CheY-GFP fusion, with less than 15% error in measured levels, by analyzing fluctuations of the fluorescence intensity (Fig. 1B).

Bacteria PS2001 strain did not tumble; motors were always in CCW state. Tumbling was restored when the CheY-GFP fusion was expressed from inducible plasmids (*19*). For a given concentration of inducer (isopropyl-β-D-thiogalactoside, IPTG), the cell-to-cell concentration [CheY-P] was widely distributed around a mean value (ranging from 0.8 to 6 μM), with the typical standard deviation of ~24% of the mean. We used three IPTG concentrations (0, 5, and 10 μM) to cover the whole range of [CheY-P] to determine the motor characteristics.

When the CW bias for individual cells was plotted versus their internal [CheY-P] (Fig. 2A), we found that the CW bias measured from different cells, preinduced with various inducer levels, fell onto the same sigmoid curve. When an induction process was followed for an individual cell, the activity of CheY-P and the GFP fluorescence were also observed to correlate (*20*). Thus, within experimental resolution, individual motors were characterized by a uniform input-output relation (*21*). This remarkable uniformity of the motor characteristics also provided an internal control of the consistency of our measurements.

The sigmoid characteristics of the flagellar motors cannot be well fitted by a Hill function in the whole range of concentrations (Fig. 2A). However, a Hill plot of our data for the bias values between 0.1 and 0.9 leads to an apparent slope of ~10.3 ± 1.1 [with dissociation constant (K) = 3.1 μM/s] (*19*, *22*). Previous experiments (*4–6*) reported much lower values for the Hill coefficient, ranging from 3.5 to 5.5. To explain this discrepancy, one should note that previous attempts to characterize flagellar motors were made by averaging the protein concentrations over cell populations. This averaging effectively smoothed out the characteristics of motors, leading to lower values of the Hill coefficient (*23*).

We measured independently the switching frequency between CW and CCW states (Fig. 2B). It was peaked strongly around [CheY-P] ~3 μM, about the same concentration for which the CW bias is equal to 0.5.

The uniformity of the motor characteristic suggests that some of the structural features of the motors may be rather tightly regulated. Physiological measurements of the behavior

[1]Departments of Physics and of Molecular Biology, Princeton University, Princeton, NJ 08544, USA. [2]Department of Microbiology and Infectious Diseases, University of Calgary, Calgary, Alberta, Canada T2N 4N1.

*To whom correspondence should be addressed. E-mail: phcluzel@phoenix.princeton.edu

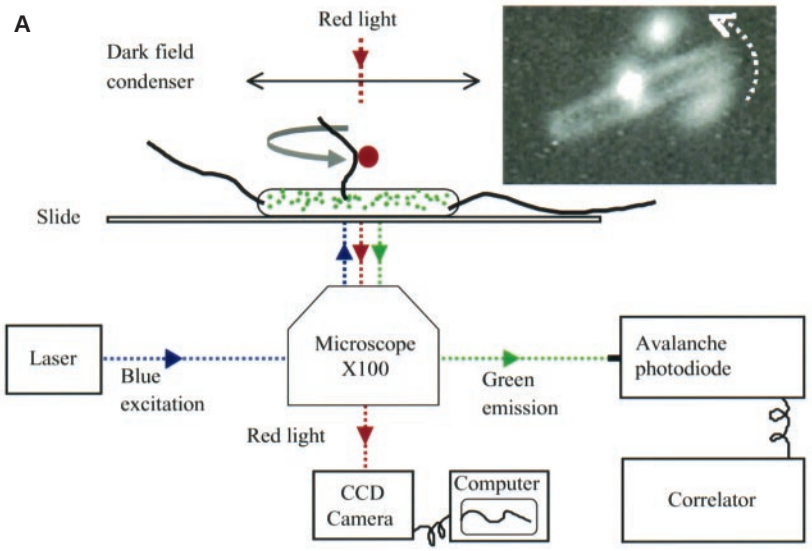

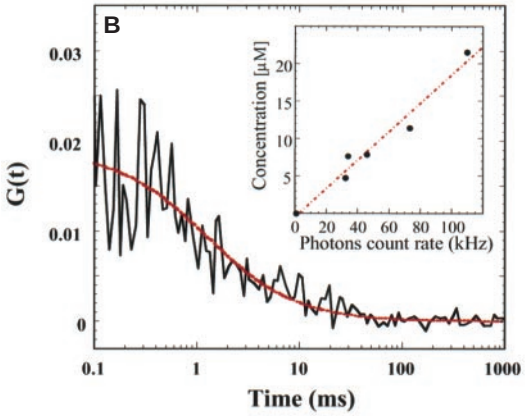

Fig. 1. (**A**) Schematic view of the experimental apparatus. We modified an inverted Zeiss microscope to perform FCS measurements on individual cells. The cell was specifically attached by its flagella onto a microscope slide. A 0.5-μm latex bead (Polyscience), attached to a flagellum with rabbit antibodies to flagellin, is used as a marker to visualize a free rotating flagellum. The CW bias was computed as the ratio of the time spent in CW to the total time duration. The FCS technique allowed us to measure GFP-tagged protein concentration in the same bacterium. The fluctuations of the total fluorescence intensity were processed in real time by a correlator (ALV-5000/E) that provided an autocorrelation function (*14*). CCD, charge-coupled device. (**Inset**) A dark-field illumination (red light) was used to record the rotation of a single flagellum of a bacterium attached to a cover slip. For clarity, only three images, 1/15 s apart, were superimposed to show the circular trajectory of the bead. [When a bead was attached to several flagella, its trajectory was no longer circular and it moved erratically. Here, the bead was rotating CCW, a state corresponding to smooth swimming (*9*)]. (**B**) Typical autocorrelation function measured for diffusing CheY-P–GFP molecules in a single cell. The amplitude of the autocorrelation function at the intercept with the vertical axis is inversely equal to the number of molecules (N) in the detection volume. We fit this function (continuous red line) with $G(t) = 1/N[1 + (4Dt/\omega^2)]^{-1}$, which describes two-dimensional translational diffusion (*15*). D is the diffusion constant of the fluorescent molecules, t is the time variable, and $2\omega = 0.3$ μm is the diameter of the detection volume in our experimental configuration; one molecule in this volume represented a concentration of 44 nM. The autocorrelation functions were measured from acquisitions of 7 s. The average diffusion constant of the cytoplasmic CheY-GFP fusion, evaluated from this fit, was 4.6 ± 0.8 $\mu m^2\ s^{-1}$ (*16*). (**Inset**) A typical calibration curve, providing a linear relation between concentration of CheY-P–GFP and the fluorescent light intensity for five individual cells. Protein concentrations on this curve were obtained with the FCS technique. We then used the calibration curve to convert fluorescence intensity into GFP concentration in those cells whose flagellar rotation was monitored. This method reduced the photobleaching of GFP by measuring the fluorescence intensity for only 0.5 s (*17*).

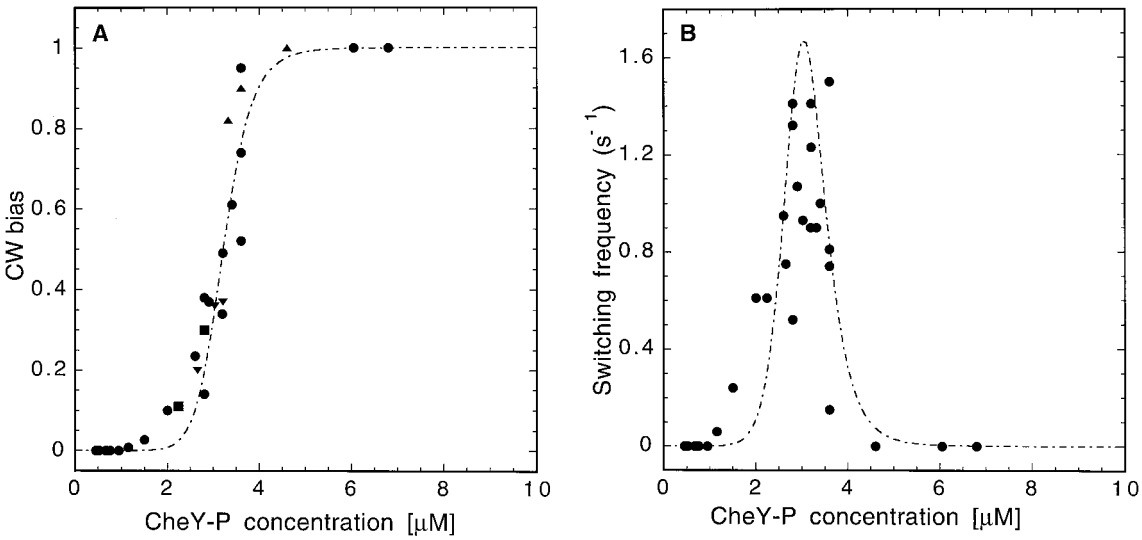

Fig. 2. (**A**) Characteristic response of individual motors as a function of CheY-P concentration. Each data point describes a simultaneous measurement of the motor bias and the CheY-P concentration in an individual bacterium. The CW bias was computed by analyzing video recordings for at least 1 min. We introduced the *cheY-gfp* (*13*) fusion gene into the strain PS2001. It is believed that in this strain, all CheY molecules are phosphorylated (*12*). Cells were grown from an overnight culture in tryptone broth at 30°C and then harvested (absorbance = 0.5 at 595 nm). To cover the whole range of motor response, we grew cells with three different IPTG concentrations (0, 5, and 10 μM) and then washed and resuspended them in minimum medium ●. The second set of experiments was also performed to check whether the folding kinetics of the GFP would affect the CheY-P activity under our experimental conditions. The expression of CheY-P–GFP fusion was monitored after the Luria-Bertoni (LB) medium was saturated with 10 mM IPTG. While the cells were expressing the CheY-P–GFP fusion, the motors' bias would increase and follow the same sigmoid curve (*21*). Time points correspond to 18, 28, and 33 min for ▼, to 60 and 69 min for ■, and to 17, 23, and 26 min for ▲, after the IPTG was added. The dashed line shows the best fit obtained with a Hill function (Hill coefficient $N_H = 10.3 \pm 1.1$ and $K_M = 3.1$ μM). Motors were locked in (CW) state for tested CheY-P concentrations ranging from ~4.6 to 25 μM (*27*). (**B**) Switching frequency, F, measured from the same cells as in (A). F was defined as the number of times that a motor switched its direction of rotation divided by the duration of the recording. In agreement with previous observations, we observe that the data points for the switching frequency are more scattered than those obtained for the motor bias (*5*). The dashed line gives the first derivative of the Hill function [from (A)] with respect to [CheY-P]. It is interesting to note that F qualitatively behaves as $F \sim [\partial(\text{CW-bias})/\partial C]$, where C is [CheY-P].

of flagellar motors cannot provide information about their molecular architecture. However, to interact with the motor, CheY-P molecules bind to a cytoplasmic FliM protein ring, consisting of ~30 binding sites (*8*, *24*). It may be that the steep input-output characteristic of motors is related to a cooperative binding process of the CheY-P molecules to the FliM subunits.

Why does the network signal transduction need such a sensitive readout to perform chemotaxis? According to the motor characteristic, a small variation in [CheY-P] leads to a large change in motor bias. Such a steep input-output relation, called ultrasensitivity (*25*), attributes to the motor the function of an amplifier. The high gain of the chemotactic signal transduction system may thus derive from functional properties of the motors (*3*). Furthermore, because of the steep input-output characteristic of the motors, the cell must adjust [CheY-P] around the operational value of 3 μM. It seems likely that an additional molecular mechanism to adjust [CheY-P] within the operational range of the motors (*26*) will exist. Such a mechanism would also help to reconcile the high amplification characteristic with a wide dynamic range of chemotactic sensitivity (*3*, *25*).

The present experiments establish that it is possible, at a single-cell level, to correlate biochemical quantities, such as intracellular protein concentrations, with cell behavior. They should be of importance not only for the understanding of chemotaxis but also for quantitative studies of a wide range of biochemical and genetic networks.

References and Notes

1. A rare example of single-cell study of biochemical networks is provided by a recent analysis of *Xenopus* oocytes, which revealed the mitogen-activated protein kinase cascade as a sharp epigenetic switch [J. E. Ferrell Jr. and E. Machleder, *Science* **280**, 895 (1998)].
2. J. L. Spudich and D. E. Koshland Jr., *Nature* **262**, 467 (1976).
3. P. A. Spiro, J. S Parkinson, H. G. Othmer, *Proc. Natl. Acad. Sci. U.S.A.* **94**, 7263 (1997).
4. U. Alon *et al.*, *EMBO J.* **17**, 4238 (1998).
5. B. E. Scharf, K. A. Fahrner, L. Turner, H. C. Berg, *Proc. Natl. Acad. Sci. U.S.A.* **95**, 201 (1998).
6. S. C. Kuo and D. E. Koshland, *J. Bacteriol.* **171**, 6279 (1989).
7. D. Bray, M. D. Levin, C. J. Morton-Firth, *Nature* **393**, 6685 (1998).
8. R. M. Macnab, in *Two Component Signal Transduction*, J. A. Hoch and T. J. Silhavy, Eds. (American Society for Microbiology, Washington, DC, 1995), pp. 181–199.
9. S. H. Larsen, R. W. Reader, E. N. Kort, W.-W. Tso, J. Adler, *Nature* **249**, 74 (1974).
10. H. C. Berg and D. A. Brown, *Nature* **239**, 500 (1972).
11. M. Welch, K. Oosawa, S. Aizawa, M. Eisenbach, *Proc. Natl. Acad. Sci. U.S.A.* **90**, 8787 (1993); R. Barak and M. Eisenbach, *Biochemistry* **31**, 1821 (1992).
12. In addition to *cheY*, this strain also lacks two other genes coding for CheB, which demethylates the receptors, and CheZ, which dephosphorylates CheY-P. Several lines of evidence from in vitro data and (*4*) indicate that, in this strain, essentially all of the CheY present in the cytoplasm is phosphorylated. To verify if the presence of the GFP modified the phosphorylation of CheY-GFP, we performed in vitro kinase assays (*27*). There is no noticeable difference between phosphorylation rates for CheY and CheY-GFP.
13. CheY-GFP was expressed under control of lacOP with the low-copy plasmid pMGS98 (CmR). This plasmid was engineered by replacing the *cheY* gene in pLC576 (*4*) with an in-frame cheY-gfp fusion constructed by polymerase chain reaction amplification of the *cheY* gene (including the ribosome binding site) and gfp#2 [B. P. Cormack, R. H. Valdivia, S. Falkow, *Gene* **173**, 33 (1996)].
14. The glass slide was coated with amino-silanes and rabbit antibodies to flagellin that were covalently cross-linked to amino-silanes with glutaraldehyde. Transitions from CW to CCW and from CCW to CW states were manually scored from slowed-down (to 1/3 speed) video recordings and recorded on charts with LabView software (National Instrument, Austin, TX). Errors on the timing of transitions were less than 0.2 s. The incident excitation light was provided by the 488-nm line of an argon laser (air-cooled ion laser 160, Spectra Physics, Mountain View, CA). The laser beam was expanded to a diameter of 4 mm, attenuated with a neutral density filter down to 0.1 mW, and fed to an oil immersion objective ×100 (numerical aperture = 1.3, Olympus Uplan FI, Melville, NY). We used a dichroic mirror (Q505LP, Chroma, Brattleboro, VT) to set up an epifluorescence illumination. The green fluorescence emission was rejected from the side of the microscope with a cold mirror (CP-SM-550, CVI, Livermore, CA). The residual blue component was filtered out from a long-pass green filter (06-515, CVI). A convergent lens focused the outcoming beam onto the core (50 μm) of a multimode optical fiber (Spectran, Sturbridge, MA). The optical fiber was connected to an avalanche photodiode (SPCM, EG&G, Quebec, Canada) that delivered a TTL pulse for each detected photon.
15. D. Magde, E. Elson, W. W. Webb, *Biopolymers* **13**, 29 (1974); E. Elson and D. Magde, *Biopolymers* **13**, 1 (1974); R. Rigler, in *Fluorescence Correlation Spectroscopy*, O. S. Wolfbeis, Ed. (Springer-Verlag, Berlin, 1992), pp. 13–24.
16. R. Brock, G. Vamosi, G. Vereb, T. Jovin, *Proc. Natl. Acad. Sci. U.S.A.* **96**, 10123 (1999).
17. This method allowed us fast and consecutive concentration measurements of cells of interest without bleaching irreversibly (less 5%) the GFP. The lower data point (0 μM) gives the amplitude of the background noise. The limit of the detection ranged from ~0.15 to 50 μM, corresponding to a background noise of three molecules and an upper limit of ~1000 molecules in the detection volume, respectively. Because of the errors in focusing and alignment of the laser spot with respect to the cell body, concentration could not be determined with precision better than 15%.
18. M. Eigen and R. Rigler, *Proc. Natl. Acad. Sci. U.S.A.* **91**, 5740 (1994); S. Maiti, U. Haupts, W. W. Webb, *Proc. Natl. Acad. Sci. U.S.A.* **94**, 11753 (1997).
19. To check whether the presence of a GFP molecule in the CheY-GFP fusion could modify the cooperativity of the binding with the motors, we analyzed, on video recordings, the swimming behavior of individual cells. Two populations of cells carrying either wild-type CheY or CheY-GFP (both expressed from the same low-copy plasmid vector) were grown under the same conditions (see Fig. 2A) and preinduced with 5 μM of IPTG. From these two populations, we reported, on two histograms, the number of cells (out of 60) having either a "smooth," "intermediate," or "tumbly" behavior. We defined these three types of behavior as "smooth" for cells having a tumbling frequency (TF) inferior to 0.1, "intermediate" when $0.1 < TF < 1$, and "tumbly" when $TF > 1$. We followed individual cells and manually scored the number of tumbles. We computed TF, for single cells, as the ratio of the number of tumbles to the duration of the recording. The two histograms were remarkably similar (*27*). This rather arduous analysis of the cell behavior provides a strong indication that the presence of a GFP molecule in the CheY-GFP fusion should not affect substantially the cooperativity of the binding to the motors and CheY phosphorylation.
20. The reported times for folding and oxidation of the chromophore of the GFP in vitro were on the order of 10 min and 1 hour, respectively [B. G. Reid and G. C. Flynn, *Biochemistry* **36**, 6786 (1997)]. We performed experiments in which CheY-GFP was preinduced to different levels for more than 1 hour and thus had time for GFP chromophore formation. For the experiments in which we followed the induction process in the single cell (Fig. 2A), the data points fell on the same curve. This suggests that chromophore oxidation and the folding of the GFP might be faster in vivo than in vitro (*28*). Our observations were also in agreement with a recent study on a series of NH_2-terminal fusions of proteins to GFP, where the folding of the chromophore was observed to be tightly coupled to the folding of the fused protein (*28*).
21. A. Ishahara, J. S. Segall, S. M. Block, H. C. Berg, *J. Bacteriol.* **155**, 228 (1983). The top curve of figure 5 in the Ishihara *et al.* article shows a high degree of correlation in the bias between two neighboring motors within the same cell. This result strongly suggests that motors are responding identically to the same signal, implying a uniformity of their functioning.
22. We calculated the Hill coefficient from the Hill plot in a standard fashion by retaining all data points with the CW bias between 0.1 and 0.9 (these limits do not necessarily correspond here to the physiologically relevant range of bacterial behavior).
23. Standard techniques of immunoblotting ignored the inherent diversity of bacteria, which is especially acute when proteins in the cells are expressed from plasmids. Variability of protein distribution within a population of cells depends on precise experimental conditions and the choice of strains, plasmids, or promoters [see, e.g., H. H. McAdams and A. Arkin, *Proc. Natl. Acad. Sci. U.S.A.* **94**, 814 (1997)]. Therefore, in all of these methods, the true output characteristic of flagellar motors was effectively convoluted with [CheY-P] distributions, leading typically to smooth-out characteristics with lower Hill coefficients. To mimic the use of immunoblots, we simulated on a computer the convolution of our data (sigmoid motors characteristic curve, Fig. 2A) with a Gaussian distribution of proteins (σ = 24% of the mean) [M. D. Levin, C. J. Morton-Firth, W. N. Abouhamad, R. B. Bourret, D. Bray, *Biophys J.* **74**, 175 (1998)]. In good agreement with our data and (*4*–*6*), we found that Hill coefficients ranging from 8 to 20 were respectively smoothed out from 3.9 to 4.2 when convoluted with such distribution. Generally, immunoblots may thus be inadequate tools for defining sharp slopes of biological switches. To check the validity of these computer simulations, we performed the same experiment as in (*4*) with wild-type CheY and CheY-GFP fusion. For several concentrations of IPTG (0, 1, 2.5, and 5 μM), the two populations of cells showed the same swimming behavior [thanks to U. Alon, these data were provided with the same setup as in (*4*)]. In both cases, wild-type CheY and CheY-GFP fusion reproduced identical results to those reported in figure 5 of (*4*) (*27*).
24. M. Welch, K. Oosawa, S.-I. Aizawa, M. Eisenbach, *Biochemistry* **33**, 10470 (1994); R. Zhao, C. D. Amsler, P. Matsumura, S. Khan, *J. Bacteriol.* **178**, 258 (1996).
25. D. E. Koshland, A. Goldbeter, J. B. Stock, *Science* **217**, 220 (1982); A. Goldbeter and D. E. Koshland Jr., *Proc. Natl. Acad. Sci. U.S.A.* **78**, 6840 (1981).
26. CheZ is a specific phosphatase interacting with CheY-P. It has recently been discovered in vitro [Y. Blat, B. Gillepsie, A. Bren, F. W. Dahlquist, M. Eisenbach, *J. Mol. Biol.* **284**, 1191 (1998)] that the CheZ activity is cooperative with respect to CheY-P and that the phosphatase activity is regulated at the level of the ratio CheY-P/CheZ interaction [B. E. Scharf, K. A. Fahrner, H. C. Berg, *J. Bacteriol.* **180**, 5123 (1998)]. It might be tempting to think that CheZ acts as a CheY-P concentration regulator. CheZ would contribute to the adjustment of the CheY-P concentration in the functioning range of the motors (3 μM). As noted by Scharf *et al.*, "the swarming abilities of both strains RP437 and AW405 suggested that the absolute values of CheY and CheZ are not as crucial for chemotaxis as their ratios" (p. 5125). Conversely, one could argue

that the natural level of expression of the CheZ gene is sufficient, without any further regulation, to dephosphorylate the right amount of CheY-P to adjust the system to the operational range of the motors.
27. P. Cluzel, M. Surette, S. Leibler, data not shown.
28. G. S. Waldo, B. M. Standish, J. Berendzen, T. C. Terwilliger, *Nature Biotechnol.* **17**, 691 (1999).
29. We thank U. Alon, N. Barkai, G. Bonnet, M. Elowitz, T. Griggs, C. Guet, T. Silhavy, J. Stock, J. Vilar, and E. Winfree for many helpful discussions and comments on the manuscript. This work was partially sponsored by the NIH. P.C. acknowledges support by a fellowship from the Program in Mathematics and Molecular Biology at the Florida State University, with funding from the NSF under grant DMS-9406348.

1 November 1999; accepted 14 January 2000

Salmonella Pathogenicity Island 2–Dependent Evasion of the Phagocyte NADPH Oxidase

Andrés Vazquez-Torres,[1] Yisheng Xu,[1] Jessica Jones-Carson,[1] David W. Holden,[2] Scott M. Lucia,[1] Mary C. Dinauer,[3] Pietro Mastroeni,[4]* Ferric C. Fang[1]†

A type III protein secretion system encoded by *Salmonella* pathogenicity island 2 (SPI2) has been found to be required for virulence and survival within macrophages. Here, SPI2 was shown to allow *Salmonella typhimurium* to avoid NADPH oxidase–dependent killing by macrophages. The ability of SPI2-mutant bacteria to survive in macrophages and to cause lethal infection in mice was restored by abrogation of the NADPH oxidase–dependent respiratory burst. Ultrastructural and immunofluorescence microscopy demonstrated efficient localization of the NADPH oxidase in the proximity of vacuoles containing SPI2-mutant but not wild-type bacteria, suggesting that SPI2 interferes with trafficking of oxidase-containing vesicles to the phagosome.

The central importance of the phagocyte NADPH (nicotinamide adenine dinucleotide phosphate) oxidase to innate host defense is vividly demonstrated in chronic granulomatous disease. Mutations in any of the subunits comprising the NADPH oxidase predispose patients to recurrent infections with fungi and bacteria, including *Salmonella* (*1*). The NADPH oxidase catalyzes the univalent reduction of oxygen to superoxide, an oxidizing species and precursor to potent antimicrobial molecules such as hydrogen peroxide, hydroxyl radical, and peroxynitrite (*2*, *3*). Pathogenic microbes have developed strategies to resist the antimicrobial effects of the NADPH oxidase, including the production of molecular scavengers, antioxidant enzymes, repair systems, and expression of specific antioxidant regulons (*2*). For example, the OxyR and SoxRS regulons enable *Escherichia coli* to resist the effects of hydrogen peroxide and superoxide, respectively (*4*). However, *S. typhimurium* does not require a functional OxyR or SoxRS regulon for virulence (*5*), suggesting that *Salmonella* may use alternative strategies to avoid exposure to high concentrations of phagocyte-derived oxidants in vivo.

A cluster of genes at centisome 30 of the *S. typhimurium* chromosome, designated *Salmonella* pathogenicity island 2 (SPI2), encodes a type III secretion system required for virulence and intracellular survival (*6*, *7*) and believed to translocate bacterial proteins into the cytosol of host cells. We have used immunodeficient mice to identify the specific host defenses targeted by products of the SPI2 genes. *Salmonella typhimurium* strains deficient at any of several SPI2 loci (*ssrA*, *ssaJ*, *ssaV*, *sseB*) (*8*) were found to be highly attenuated for virulence in C57BL/6 mice (Fig. 1A) (*9*). Virulence of these SPI2-mutant strains was not restored by administration of aminoguanidine, an inhibitor of inducible nitric oxide synthase (iNOS) (*10*), or by genetic abrogation of interferon-γ (IFN-γ) (*11*) or interleukin-12 (*12*) production (Fig. 1, B and C). In contrast, all four SPI2 mutants were able to cause lethal infection of congenic C57BL/6 mice deficient in the gp91*phox* subunit of the phagocyte NADPH oxidase (gp91*phox* knockout mice) (*13*) (Fig. 1D). Thus the SPI2 genes are not required for virulence in the absence of a phagocyte respiratory burst and might play a specific role in avoiding bacterial interaction with the NADPH oxidase.

Killing of isogenic *S. typhimurium* strains carrying mutations in various SPI2 genes (*ssaJ*, *sseA*, *sseB*, *ssrA*) was examined in macrophages from wild-type or respiratory burst-deficient mice (*14*). SPI2-mutant bacteria had increased susceptibility to killing by periodate-elicited murine peritoneal macrophages from C57BL/6 mice (Fig. 2A), but this enhanced

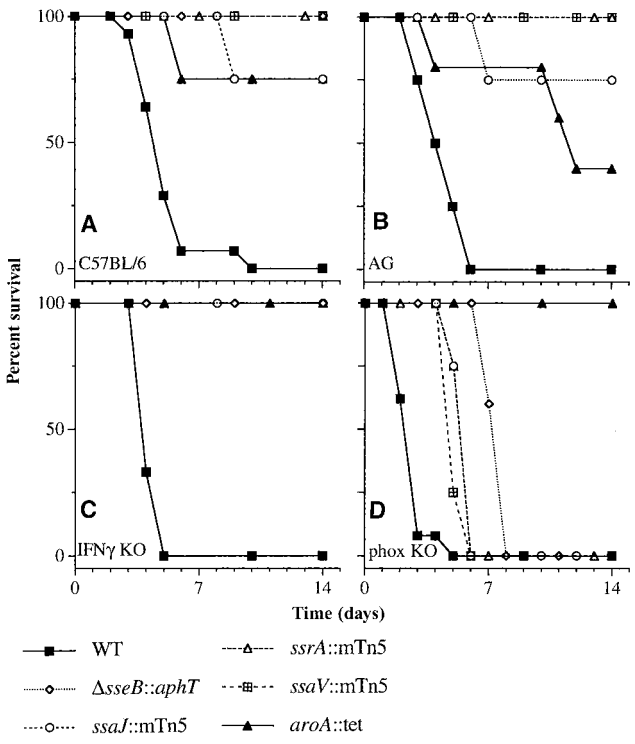

Fig. 1. Abrogation of the NADPH phagocyte oxidase restores virulence to SPI2-deficient *S. typhimurium* mutants. Survival curves are shown for wild-type C57BL/6 mice (**A**), wild-type mice fed drinking water containing the iNOS inhibitor aminoguanidine (**B**), congenic immunodeficient IFN-γ knockout mice (**C**) or gp91*phox* knockout mice (**D**), following intraperitoneal challenge with wild-type *S. typhimurium* or isogenic strains with mutations at *ssaJ*::Tn5, *ssaV*::Tn5, *ssrA*::Tn5, or Δ*sseB*::*aphT*. An isogenic *aroA*-mutant *S. typhimurium* strain with attenuated virulence in mice (*29*) was included as an additional control. These experiments used 4 to 14 mice per group.

[1]Departments of Medicine, Pathology, and Microbiology, University of Colorado Health Sciences Center, Denver, CO 80262, USA. [2]Department of Infectious Diseases, Imperial College School of Medicine, London W12 ONN, UK. [3]Indiana University School of Medicine, Indianapolis, IN 46202, USA. [4]Department of Biochemistry, Imperial College of Medicine and Technology, London SW7 2BZ, UK.

*Present address: Centre for Veterinary Science, University of Cambridge, Cambridge CB3 0ES, UK.
†To whom correspondence should be addressed. E-mail: ferric.fang@uchsc.edu